

# Many-body resonant tunneling in the Wannier-Stark system

Carlos A. Parra-Murillo,<sup>1</sup> Javier Madroño,<sup>2</sup> and Sandro Wimberger<sup>1</sup>

<sup>1</sup>*Institut für Theoretische Physik and Center for Quantum Dynamics,  
Universität Heidelberg, 69120 Heidelberg, Germany*

<sup>2</sup>*Physik Department, Technische Universität München, 85747 Garching, Germany*

We study an experimentally realizable paradigm of a complex many-body quantum system, a two-band Wannier-Stark model, for which diffusion in Hilbert space as well as many-body Landau-Zener processes can be engineered. A clean cross-over between regular to quantum chaotic spectra is found within the many-level avoided crossings at resonant tunneling conditions. The spectral properties determine the evolution of states across a cascade of Landau-Zener events, which can be used to study diffusion and to dynamically prepare target states interesting for experimental applications.

PACS numbers: 03.65.Xp, 37.10.Jk, 05.45.Mt, 71.35.Lk

*Introduction.* The rapid development of high precision techniques for the experimental control of ultracold quantum gases offers a clean way to study static and dynamical properties of interacting many-body lattice systems [1, 2]. Of particular interest are realizations of strongly correlated or complex systems of many particles. Aspects of integrability of such quantum systems are crucial for predictions, for instance, of their thermalization [3, 4]. Moreover, experiments controlling the populations of higher orbitals and bands in periodic potentials are at hand now [5, 6], which allow for the study of complex many degree-of-freedom systems.

In this Letter we present a case study of a complex many-body system including two strongly coupled energy bands. As we sketch below it can readily be realized experimentally with ultracold bosons in accelerated (or equivalently tilted) optical lattices [7]. Our system is a generic model for which the dynamics can be steered by the parameters (tilt, interaction strength, potential depth), thus implementing very different dynamics. While the mean-field transport (weakly interacting limit) is well known for this system [7, 8], even the simplest many body version, a one-band Bose-Hubbard model with(out) tilt, allows one to change between regular and quantum chaotic evolutions [9–12]. Our system is a paradigm for which, depending on the choice of parameters, full complexity in the interband transport and thermalization in Hilbert space can be reached.

Strongest interband coupling occurs at resonantly enhanced tunneling (RET) between the two bands [8, 13], where we find a crossover from regular to quantum chaotic spectral statistics with increasing density of states. These complex energy spectra determine the transport across the many avoided crossings at RET when the force  $F$  is varied. This not only generalizes results on the weakly interacting limit [14], but relates to the largely open problem of many-body Landau-Zener processes in the presence of strong particle interactions [11, 15, 16]. As two direct applications we show how the spectral properties influence the diffusion in Hilbert space, and, moreover, how to prepare target states with a high fidelity in the upper band by controlled sweeps of  $F(t)$  through the RET regime.

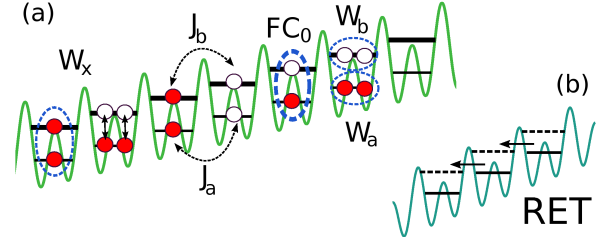


FIG. 1: (Color online) The system: (a) Many-body processes of the two-band Bose-Hubbard Hamiltonian for a bichromatic one dimensional tilted optical lattice. (b) **R**esonant **E**nhanced **T**unneling (RET) condition for the nearest neighboring double wells, i.e., for a first order resonance.

*The two-band system.* Single-particle energy bands are nowadays routinely engineered in experiments using a bichromatic optical lattice  $V(x) = -V_0 [\cos(2k_L x) + s_0 \cos(4k_L x + \phi)]$ ,  $k_L$  being the recoil momentum [17]. Choosing, e.g., the relative phase  $\phi \equiv \pi$  and appropriate values of  $s_0 = V_d/V_0$  we have a situation for which the lowest two energy bands are well separated from all higher bands [18]. An additional Stark force stimulates the quantum transport along the lattice [7, 8, 10, 11, 14] and, at the same time, it couples the bands. In the single particle picture, this coupling is maximal at specific tilts  $F_r \approx \Delta_g/2\pi r$ ,  $\Delta_g$  being the energy gap between the two bands. At those values RET occurs between levels distancing  $r$  double wells, see Fig. 1, and the integer  $r$  is called the order of the resonance [8]. The corresponding many particle problem can be described in the tight-binding limit by a two-band Bose-Hubbard Hamiltonian

$$\begin{aligned} \hat{H} = & \sum_{\alpha=a,b} \sum_{l=1}^L \frac{J_\alpha}{2} (\alpha_{l+1}^\dagger \alpha_l e^{-i2\pi F t} + h.c.) + \frac{W_\alpha}{2} n_l^\alpha (n_l^\alpha - 1) \\ & + \sum_{l=1}^L \frac{W_x}{2} (b_l^\dagger b_l^\dagger a_l a_l + h.c.) + FC_0 (b_l^\dagger a_l + h.c.) \\ & + \sum_{l=1}^L 2W_x n_l^a n_l^b + \Delta_g n_l^b, \end{aligned} \quad (1)$$

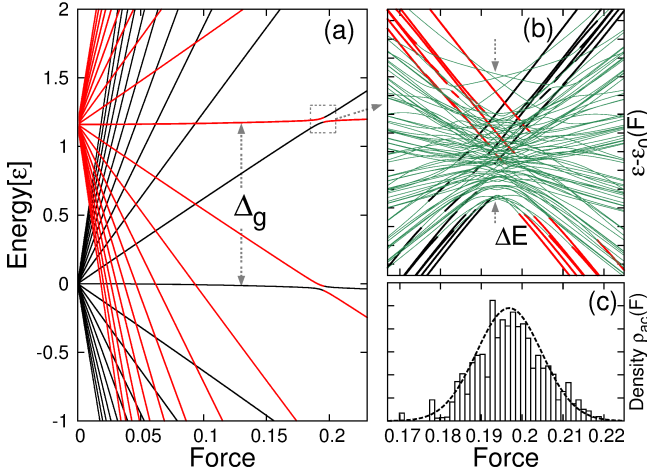


FIG. 2: (Color online) The spectrum: (a) Wannier-Stark ladders from two bands for the single particle case, with gap  $\Delta_g \approx 1.61$  at  $V_0 = 5$  and  $s_0 = 2$ . Avoided crossings appear at the resonances  $F_{r=1} = 0.1934$  with width  $\Delta_r \ll \Delta_g$ . (b) The many-body spectrum revealing the local complex structure of many avoided crossings even for this relatively small system ( $N/L = 5/3$ ).  $\varepsilon_0(F)$  is the  $F$  dependent center of the FZ. The manifolds discussed in the text are best visible on the very right as quasi-equidistant bunches of states. (c) Normalized density of avoided crossings  $\rho_{ac}(F)$  in the vicinity of  $F_{r=1}$  as a histogram and a Gaussian fit to it (dashed line).

where the bosonic annihilation (creation) operators at the  $l$ -th site are  $\alpha_l(\alpha_l^\dagger)$ , and the number operators are  $n_l^\alpha = \alpha_l^\dagger \alpha_l$ , with band index  $\alpha$ .  $J_{\alpha=a,b}$  are the hopping amplitudes, and the on-site interparticle interaction per band has a strength  $W_\alpha$ . The coupling between the bands is given by the repulsive interaction  $W_x$  at simultaneously occupied sites (see Fig. 1(a)), and by the *dipole-like* term with strength  $FC_0$  [14]. The latter coupling modifies the above resonance formula to  $F_r = \Delta_g/2\pi\sqrt{r^2 - 4C_0^2}$  by taking into account the Stark shift of the levels [14]. The prefactors in (A1) are computed based on the single-particle Wannier functions  $\psi_\alpha(x) = \langle x | \psi_\alpha \rangle$  localized within each site (i.e. within each double well), given the band structure parameters  $V_0$  and  $s_0$  [11]. Imposing periodic boundary conditions in space, the Hamiltonian (A1) is translationally invariant. In addition, it is periodic in time,  $\hat{H}(t + T_B) = \hat{H}(t)$ , with the Bloch period  $T_B = 1/F$ . This allows us to work with the Floquet Hamiltonian  $\hat{H}_f = \hat{H}(t) - i\partial_t$ , which is numerically diagonalized by a Lanczos algorithm [19]. This procedure is equivalent to diagonalize the evolution operator integrated over one Bloch period  $\hat{U}(T_B, 0) = \hat{T} \exp[-i \int_0^{T_B} \hat{H}(t) dt]$ , where  $\hat{T}$  is the time ordering operator. The quasienergies (eigenvalues of  $\hat{H}_f$ ) lie within the so-called Floquet zone (FZ) of width  $\omega_B = 2\pi F$ . The extended spectrum is thus given by the operation  $\varepsilon \rightarrow \varepsilon + n\omega_B$ , with the index  $n$  of the FZ. For  $N$  atoms, the number of quasienergies is given by

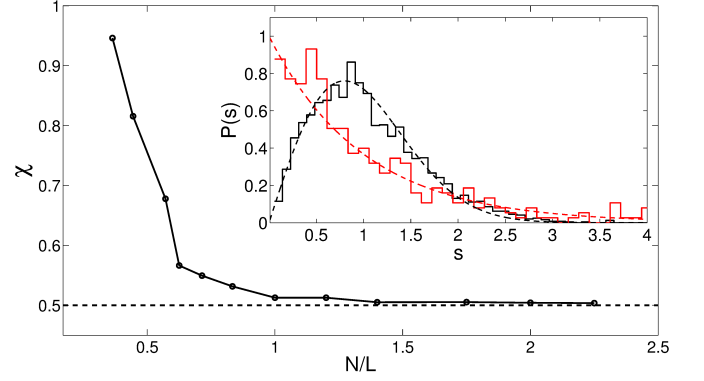


FIG. 3: (Color online) Regular-to-chaotic transition: The main panel shows  $\chi$  as a function of the filling factor  $N/L$ . Inset:  $P(s)$  before (red/grey solid line:  $N/L = 4/7$ ) and after (black solid line:  $N/L = 9/4$ ) the saturation of  $\chi$ . The dashed lines show the Poisson (red/grey) and Wigner-Dyson (black) predictions respectively. The parameters are  $V_0 = 5 = s_0$  and  $F_{r=2} = 0.0124$ .

$\mathcal{N}_s = (N + 2L - 1)!/[LN!(2L - 1)!]$ , considering the reduction by a factor  $L$  arising from the periodic boundary conditions [10], yet the effective dimension of  $\hat{H}_f$  is much larger:  $\mathcal{N}_s \Delta k$ , with  $\Delta k = 10 \dots 50$  Floquet blocks.

The force is our control parameter to analyze the spectrum in the plane  $\varepsilon$ - $F$  as shown in Fig. 2(a) for the single particle case. The gap  $\Delta_g$ , typically the largest energy scale in Eq. (A1) for a realization as shown in Fig. 1, allows us to split up the spectrum into subsets of states, each labeled by the number of particles in the upper band  $N_b$ . In the off-resonant regime, where  $F$  is not close to  $F_r$ , these subset manifolds do not mix and the levels of the various manifolds move parallel with  $F$ . Here we have approximately  $\hat{H} \approx \oplus_{N_b=0}^N \hat{H}_{N_b}$  with an energetic separation between the lowest states in energy from the nearest manifolds given by  $\Delta_r \simeq \Delta_g \sqrt{(1 - F/F_r)^2 + 4F^2 C_0^2 / \Delta_g^2}$  (see appendix). These manifolds mix, however, strongly in the vicinity of  $F_r$ , where the spectrum shows a large number of avoided crossings, see Fig. 2(c). The density of avoided crossings  $\rho_{ac}(F)$  sensitively depends on the filling factor of the lattice  $N/L$  and the interband repulsive interaction  $W_x$ . The effective region of manifold mixing, the RET regime, is that range of  $F$  for which the area under the curve  $\rho_{ac}(F)$  is visibly different from zero. There  $N_b$  is no longer a good quantum number as shown in Fig. 2(b). Here even the identification of the otherwise most distant manifolds  $N_b = 0$  and  $N_b = N$  is difficult due to the strong level mixing.

*Regular-to-chaotic transition.* The complexity of the spectra is now further investigated by means of the level spacing (or local gap) distribution  $P(s_i)$  with  $s_i = E_{i+1} - E_i$ , where  $\langle s_i \rangle = 1$ , after an appropriated unfolding procedure [12, 20]. Squeezing more many-body levels into a single FZ leads to a crossover between regular (Poisson) and quantum chaotic (Wigner-Dyson) statistics of  $P(s)$ . The number of levels can be increased by

varying the filling factor  $N/L$ , and the width of the FZ by the order  $r$  of the resonance. The parameter  $s_0$  controls the single particle band gap and the manifold splitting  $\Delta_r$ . As the manifolds approach each other more and more in the RET region, nontrivial level statistics are observed in the range  $\Delta E$  of the spectrum, with the many avoided level crossings around  $F_r$  (see Fig. 2(b)). Strong mixing of levels and long-range spectral correlations occur as soon as  $\Delta E$  becomes of the order of  $\omega_B$  as  $N/L$  increases. Here we observe Wigner-Dyson statistics in  $P(s)$ , see the inset in Fig. 3, and a logarithmic scaling of the level-level correlation function  $\Sigma^2$  [20] (not shown here). To estimate the critical parameters, at which the crossover is reached, we propose to study the distribution of the energies in  $\Delta E$  by means of the quantity

$$\chi \equiv \int_{FZ} \rho^2(\varepsilon) d\varepsilon / \left[ \int_{FZ} \rho(\varepsilon) d\varepsilon \right]^2, \quad (2)$$

with  $\rho(\varepsilon)$  being the level density of the rescaled energies  $\varepsilon' \rightarrow 2\varepsilon/\omega_B$ .  $\chi$  characterizes the distribution of the levels in energy space. This function saturates to  $\chi_{\min} = 1/2$ , if  $N_s$  is large enough and the energies are uniformly distributed over the entire FZ. This latter is a signature of chaotic spectra. Otherwise  $\chi$  is larger than this saturation value and diverges if  $\Delta E \ll \omega_B$ . Fig. 3 shows that the saturation value is reached around  $(N/L)_c \sim 1$ . In this spectral analysis we do not take into account those systems for which the greatest common divisor  $\gcd(N, L)$  is larger or equal to one, due to the existence of a temporal symmetry of the Hamiltonian as reported in [10]. In the following we discuss important consequences that emerge from the spectral characteristics in the RET regime.

*Level diffusion.* The structure of avoided crossings presented above provides a perfect setup to study dynamical processes arising from a cascade of Landau-Zener (LZ) events in the many-body spectrum around  $F_r$ . We first focus on the diffusion process triggered by the parametric-time evolution of individual eigenstates  $|\varepsilon_i\rangle$  with  $F(t) = F_0 + \alpha t$ , and  $\alpha = \Delta F/\Delta T$ .  $\Delta F$  is the effective extension of the RET regime and  $\Delta T \gg T_B$  is the time of the evolution from the starting tilt  $F_0$  to the final value  $F_f$ . The temporal dependence of  $F(t)$  in Eq. (2) breaks the time periodicity of the Hamiltonian. In consequence, we must compute now the temporal evolution explicitly, e.g., by using a fourth-order Runge-Kutta method. Let  $|\Phi_m(0)\rangle$  be one of the eigenstates at fixed  $F_0 = F_r - \Delta F/2$ . To quantify the diffusion in energy space we compute the projections  $C_i(t) \equiv \langle \varepsilon_i(F_k) | \Phi_m(t) \rangle$ , where  $|\varepsilon_i(F_k)\rangle$  are the eigenstates at the instantaneous tilt  $F(t) = F_k$ . As a function of the local energies, the distribution of coefficients  $\{|C_i(t)|^2\}$  is just the *local density of states* (LDOS)  $P_m(\varepsilon, t) = \sum_i |C_i(t)|^2 \delta(\varepsilon - \varepsilon_i)$  [4, 21]. At  $F_0$ ,  $P_m(\varepsilon, 0)$  is  $\delta$ -shaped but as the tilt increases with time, it delocalizes because of the many LZ processes. This effect depends on  $\alpha$  and sensitively on the type of statistical distribution of the spectrum close to  $F_r$ . This is shown in Fig. 4 (right

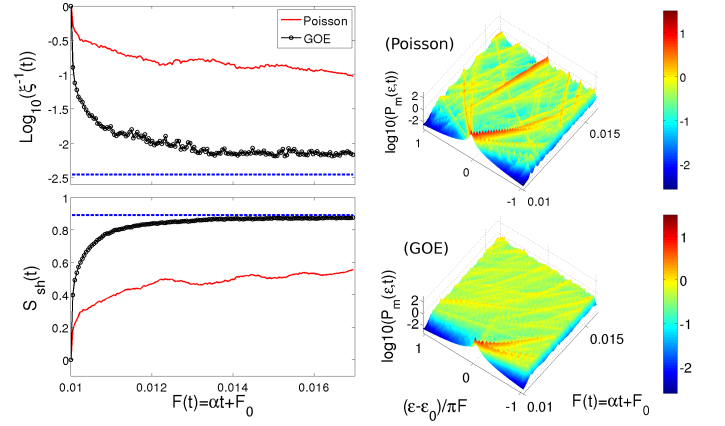


FIG. 4: (Color online) Diffusion: (left panel) Averaged  $\xi^{-1}(t)$  and  $S_{\text{sh}}(t)$  for  $\alpha = 1.12 \times 10^{-3}$ . The blue dashed lines represent the maximal delocalization value predicted by random matrix theory (see main text). (right panel) Temporal evolution of eigenstates of type  $N_b = 2$  and  $N_b = 3$  through a Poisson-distributed spectrum ( $N/L = 5/6$ ) and a GOE-distributed one ( $N/L = 7/4$ ), respectively. The remaining parameters are  $r = 2$  for  $V_0 = 5 = s_0$ .

panels) for two generic spectra corresponding to the fillings  $N/L = 5/6$  and  $N/L = 7/4$ , which are Poisson- and GOE-distributed respectively. We characterize the spreading over the spectrum quantitatively by the inverse participation ratio [21] and the Shannon entropy [9]:

$$\xi^{-1}(t) \equiv \left\langle \sum_{i=0}^{N_s-1} |C_i(t)|^4 \right\rangle_m \quad (3)$$

$$S_{\text{sh}}(t) \equiv \left\langle -\frac{1}{\log_{10}(N_s)} \sum_{i=0}^{N_s-1} |C_i(t)|^2 \log_{10}(|C_i(t)|^2) \right\rangle_m \quad (4)$$

with the average taken over a large set of similar initial conditions. For the Poissonian case we consider the ensemble of initial states that lie in the manifold  $N_b = 2$  ( $N/L = 6/5$ ), whilst for the GOE case those from the manifold  $N_b = 3$  ( $N/L = 7/4$ ). The number of accessible eigenstates is  $N_s(5/6) = 728$  and  $N_s(7/4) = 858$ . Complete delocalization occurs as the coefficients  $\{|C_i|^2\}$  fluctuate around the equipartition condition for thermalization  $|C_i(t)|^2 = 1/N_s$ . Here the localization measures slowly converge to the values  $\log_{10}(\xi^{-1}) \approx \log_{10}(3/N_s) \approx -2.41$  and  $S_{\text{sh}} \approx \log_{10}(0.48N_s)/\log_{10}(N_s) \approx 0.88$  predicted by random matrix theory [4]. It is thus clearly seen that in the course of the evolution, the system undergoes a dynamical diffusion (see Fig. 4) through the accessible Hilbert space. This diffusive spread is much stronger for a GOE spectrum  $\mu \simeq 94\%$  than for a Poissonian  $\mu \simeq 40\%$ , where  $\mu$  is the percentage of delocalization at final time  $\Delta T$  with respect to the maximal possible delocalization defined above.

Hence the temporal evolution of a given initial state when sweeping  $F(t)$  across the RET regime sensitively depends on the spectral properties of the system. Strong

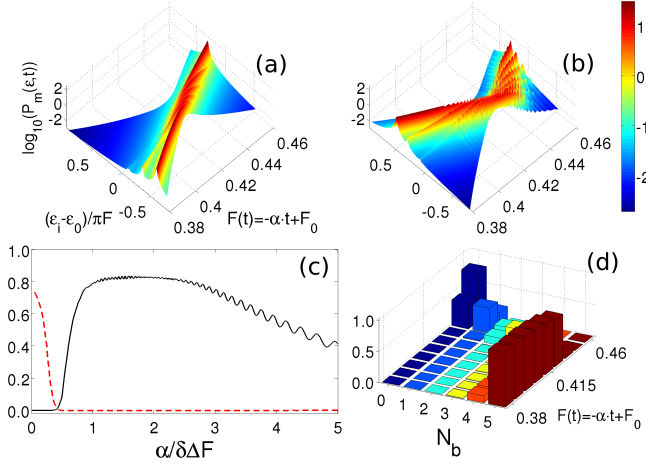


FIG. 5: (Color online) State preparation: Evolution of the eigenstate  $|\Phi_0(0)\rangle \approx |11111; 00000\rangle$  with (a)  $\alpha/\delta\Delta F = 50$  and (b)  $\alpha/\delta\Delta F = 1.9$  from  $F_f = 0.46$  to  $F_0 = 0.38$ . (c) Success probability  $P_{\text{tar}}$  for the target state  $|\Phi_f(\Delta T)\rangle = |00000; 11111\rangle$ , with  $N/L = 5/5$  (solid line) and survival probability of the initial states  $|\Phi_0(0)\rangle \approx |11111; 00000\rangle$  (dashed line). (d) Instantaneous manifold occupation  $P(N_b) = |\hat{P}_{N_b}|\Phi(t)\rangle|^2$ .  $\alpha/\delta\Delta F = 1.9$  in (c) and (d).

diffusion along the spectrum occurs for quantum chaotic (Wigner-Dyson distributed), for which the instantaneous LDOS  $P_m(\varepsilon, t)$  is uniform in the entire FZ since  $|C_i(t)|^2 \approx 1/\mathcal{N}_s$ , whilst a full spreading over all levels is prohibited by regular (Poisson) spectra. In the latter case,  $P_m(\varepsilon, t)$  is typically described by the *Breit-Wigner* formula [22] for  $t > 0$  as shown in Fig. 4 (upper right panel).

*State preparation.* The knowledge of the diffusion properties presented above allows us to prepare specific target states with high fidelity. We concentrate now on the case of regular spectra since for them a simple linear sweep of the tilt can be used to control the respective evolution. This is a consequence of the coupling of smaller subsets of levels as compared to GOE-distributed spectra. An extension to the GOE case seems possible, yet with more complicated pulses  $F(t)$  due to the many energy scales present in the problem (see also conclusions below). The following analysis is made around the resonance at  $F_{r=1} = 0.4248$  for  $V_0 = 5$  and  $s_0 = 1$ .

Outside the RET regime, our Floquet eigenstates can be identified since they essentially correspond to specific translationally invariant Fock states in real space. For the following examples, we start our parametric evolution with initial Mott-insulator-like states of the untilted problems:  $|\Phi_0(t=0)\rangle \approx |111\dots; 000\dots\rangle$ . The target state  $|\Phi_f(\Delta T)\rangle = |000\dots; 111\dots\rangle$  is of particular interest for experiments, since its preparation is difficult without applying additional complications (e.g. photon-assisted transitions [23]). Depending on the wanted target state we can adapt the rate of the linear sweep  $F \propto t$  across the RET regime. For given  $F_r$  and  $\Delta E$  (see above), the average mean level spacing is  $\delta = \Delta E/\mathcal{N}_s$ , which determines the time scale of the sweep rate. For  $\alpha \gg 1$  we

expect to follow the diabatic arm of the single particle avoided crossing in Fig. 2(a). In our many-body setting, the corresponding final state is then close to a state of the  $N_b = 0$  manifold, i.e., to a state where all particles are in the lower band. On the other hand for  $\alpha \approx \delta\Delta F$ , we expect an adiabatic crossing, implying a strong final occupation of the high lying manifolds  $N_b = N - 1$  and  $N_b = N$  (see Fig. 5(b)).

For the preparation of the different target states we use the the following protocol: (i) the system is prepared in the state  $|\Phi_0(0)\rangle = |11111, 00000\rangle$  in the flat lattice with  $N/L = 5/5$ . (ii) A sudden sweep ( $\alpha \gg 1$ ) from  $F = 0$  to  $F_f > F_r$  is applied, which leaves the system unchanged with high fidelity. (iii) This latter state is evolved back from  $F_f$  to  $F_0 < F_r$  by a controlled sweep  $F(t) = F_f - \alpha t$  with relatively small  $\alpha$ . Finally, (iv), at  $t = \Delta T$ , we compute the success probability of the target state in the upper band defined by  $P_{\text{tar}} \equiv |\langle 00000; 11111 | \hat{U}(\Delta T, 0) | \Phi_0(0) \rangle|^2$ . This probability is shown in Fig. 5(c) (solid line), as a function of  $\alpha$  rescaled by  $\delta\Delta F$ . It is seen that  $P_{\text{tar}}(\alpha)$  has a plateau around  $\alpha_c \approx 2\delta\Delta F$ , reaching a value  $P_{\text{tar}} \approx 0.81$ . The dashed line corresponds to the survival probability  $P_{\text{surv}}(\alpha)$  of the initial condition. It is particular illuminating to use the above introduced manifolds to picture the evolution of the many-body states during the sweep. Fig. 5(d) nicely shows the transformation of the  $N_b = 0$  manifold to states living essentially in the  $N_b = N$  manifold. Imperfections in the preparation arise particularly from the  $N_b = N - 1$  contribution visible in the manifold distribution at the final time.

*Conclusions.* We have studied the spectral properties of an experimentally realizable paradigm of a complex many-body quantum system, for which the spectra show a regular to chaotic transition. The spectral characteristics can be probed by sweeping across the resonant region using the Stark force as a control parameter. This allows us not only predictions on the diffusion of our many-body system in Hilbert space, yet as an important application also the preparation of target states with high fidelity. The latter may be increased even further by applying methods of coherent control for our many-body quantum system [24]. In the chaotic regime, such an optimal pulse control is definitely needed to steer the state diffusion. Our results open a route to engineer complex many-body systems at will, with immediate experimental implications [6, 15, 25].

*Acknowledgments.* CPM and SW acknowledge financial support from the DFG (FOR760), the Helmholtz Alliance Program EMMI (HA-216), and the HGSFP (GSC 129/1). We are grateful to F. Borgonovi, A. Buchleitner, P. Schlagheck and A. Tomadin for lively discussions.



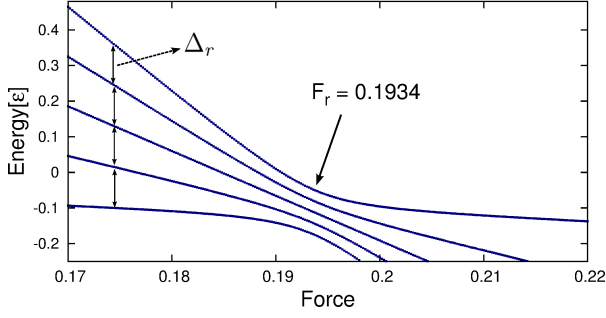


FIG. 6: Noninteracting many-body spectrum around  $F_r = 0.1934$ , at  $\Delta_g = 1.609$ ,  $V_0 = 5$  and  $s_0 = 2$ , c.f. Fig. 2 in the paper.

### Appendix A: Manifolds far from resonance and derivation of manifold energy distance

Here we motivate the manifold energy scaling defined in the main text. Let us begin with the noninteracting version of the time-independent Hamiltonian, Eq. (1) of the paper,

$$\hat{H} = \sum_{\alpha=a,b} \sum_{l=1}^L \left[ \frac{J_\alpha}{2} (\alpha_{l+1}^\dagger \alpha_l + h.c.) + F l n_l^\alpha \right] + \sum_{l=1}^L \left[ \Delta_g n_l^b + F C_0 (b_l^\dagger a_l + h.c.) \right], \quad (\text{A1})$$

which, for  $F = 0$ , is easily diagonalized in momentum space. The eigenenergies are given by  $\varepsilon_{F=0, N_b} = N_b \Delta_g + \varepsilon_0^{(L)}$ , where  $N_b$  is the total number of particles

in the upper band  $N_b = \langle \sum_l n_l^b \rangle$ . The quantum numbers  $N_b$  define sets of  $M(N_b)$  degenerate states, where  $\sum_{N_b} M(N_b) = \mathcal{N}_s L$ . These sets we call manifolds. As  $F$  increases, single energy levels from the different manifolds (corresponding to different  $N_b$ ) try to cross at specific tilts  $F_r$ , which defines the resonantly enhanced tunneling (RET) regime. Note that the transition between neighboring manifolds arises from the single particle transition term  $FC_0$ . This latter single-particle process, at RET conditions, can be studied by reducing the full Floquet matrix to the resonantly coupled terms only, given by an effective  $2 \times 2$  Hamiltonian matrix [26]. Therefore the energy differences between the manifolds  $|N_b\rangle$  and  $|N_b + 1\rangle$  can be estimated by diagonalizing the corresponding  $2 \times 2$  matrix

$$H_{2 \times 2} = \begin{pmatrix} \varepsilon_{F, N_b+1} & FC_0 \\ FC_0 & \varepsilon_{F, N_b} \end{pmatrix}. \quad (\text{A2})$$

The energies  $\varepsilon_{F, N_b}$  are proportional to  $F$  by the simple geometric relation  $\varepsilon_{F, N_b} - \varepsilon_0 = \frac{N_b \Delta_g}{F_r} (F_r - F)$  (see Fig. 6). Thus, by diagonalizing  $H_{2 \times 2}$ , we see that the energy difference  $\Delta_r$  shown in Fig. 6 is

$$\begin{aligned} \Delta_r &= \sqrt{(\varepsilon_{F, N_b+1} - \varepsilon_{F, N_b})^2 + 4FC_0^2} \\ &= \Delta_g \sqrt{(1 - F/F_r)^2 + 4FC_0^2/\Delta_g^2}. \end{aligned} \quad (\text{A3})$$

The interparticle interaction now splits up the internal manifold levels and a strong mixing occurs at RET conditions when the levels come closest, see Fig. 6 here and Fig. 2 of the paper.

- 
- [1] M. Lewenstein, A. Sanpera, V. Ahufinger, B. Damski, A. Sen De, and U. Sen, *Adv. Phys.* **56**, 243 (2007); I. Bloch, J. Dalibard, and W. Zwerger, *Rev. Mod. Phys.* **80**, 885 (2008).
  - [2] J. Simon, S. Bakr, M. Ruichao, M. E. Tai, M. Preiss and M. Greiner, *Nature* **472**, 307 (2011); C. Weitenberg, M. Endres, J. F. Sherson, M. Cheneau, P. Schauß, T. Fukuhara, I. Bloch, and S. Kuhr, *Nature* **471**, 319 (2011).
  - [3] A. Altland and F. Haake, *Phys. Rev. Lett.* **108**, 073601 (2012); M. Rigol and M. Srednicki, *ibid.* 110601.
  - [4] L. F. Santos, F. Borgonovi, and F. M. Izrailev, *Phys. Rev. Lett.* **108**, 094102 (2012); *Phys. Rev. E* **85**, 036209 (2012).
  - [5] M. Köhl, H. Moritz, T. Stöferle, K. Günter, and T. Esslinger, *Phys. Rev. Lett.* **94**, 080403 (2005); G. Wirth, M. Ölschläger, and A. Hemmerich, *Nature Phys.* **7**, 147 (2010); M. Ölschläger, G. Wirth, T. Kock, and A. Hemmerich, *Phys. Rev. Lett.* **108**, 075302 (2012).
  - [6] T. Müller, S. Fölling, A. Widera, and I. Bloch, *Phys. Rev. Lett.* **99**, 200405 (2007).
  - [7] O. Morsch and M. Oberthaler, *Rev. Mod. Phys.* **78**, 179 (2006); E. Arimondo and S. Wimberger, *Tunneling of ultracold atoms in time-independent potentials*, in *Dynamical Tunneling*, S. Keshavamurthy and P. Schlagheck (Eds.), Taylor & Francis – CRC, Boca Raton (2011).
  - [8] C. Sias, A. Zenesini, H. Lignier, S. Wimberger, D. Ciampini, O. Morsch, and E. Arimondo, *Phys. Rev. Lett.* **98**, 120403 (2007); A. Zenesini, H. Lignier, G. Tayebirad, J. Radogostowicz, D. Ciampini, R. Mannella, S. Wimberger, O. Morsch, and E. Arimondo, *Phys. Rev. Lett.* **103**, 090403 (2009).
  - [9] A. R. Kolovsky, A. Buchleitner, *EPL* **68**, 632 (2004).
  - [10] A. Buchleitner and A. R. Kolovsky, *Phys. Rev. Lett.* **91**, 253002 (2003); A. R. Kolovsky, H.J. Korsch, and E.-M. Graefe, *Phys. Rev. A* **80**, 023617 (2009).
  - [11] A. Tomadin, R. Mannella, and S. Wimberger, *Phys. Rev. Lett.* **98**, 130402 (2007); *Phys. Rev. A* **77**, 013606 (2008).
  - [12] P. Buonsante and S. Wimberger, *Phys. Rev. A* **77**, 041606(R) (2008).
  - [13] M. Glück, A. R. Kolovsky, and H. J. Korsch, *Phys. Rep.* **366**, 103 (2002).
  - [14] P. Plötz, J. Madroñero, and S. Wimberger, *J. Phys. B.* **43**, 08001(FTC) (2010); P. Plötz, P. Schlagheck, and S. Wimberger, *Eur. Phys. J. D* **63**, 63 (2011).
  - [15] Yu-Ao Chen, S. D. Hubber, S. Trotzky, I. Bloch, and E.

- Altman, Nature Phys. **7**, 1801 (2010).
- [16] D. Witthaut, E. M. Graefe, and H. J. Korsch, Phys. Rev. A **73**, 063609 (2006); A. Altland and V. Gurarie, Phys. Rev. Lett. **100**, 063602 (2008).
  - [17] T. Salger, C. Geckeler, S. Kling, and M. Weitz, Phys. Rev. Lett. **99**, 190405 (2007).
  - [18] B. M. Breid, D. Witthaut, and H. J. Korsch, New J. Phys. **8**, 110 (2006).
  - [19] C. Lanczos, J. Res. Nat. Bur. Standards, Sec. B **45**, 225 (1950); A. Buchleitner, D. Delande, and J.C. Gay, J. Opt. Soc. Am. B **12**, 520 (1995).
  - [20] F. Haake, Quantum signatures of chaos (Springer, Heidelberg, 2010).
  - [21] T. Dittrich and U. Smilansky, Nonlinearity **4**, 54 (1991).
  - [22] G. Breit and E. Wigner, Phys. Rev. **49**, 519 (1936); M. Klein, D. Robert, and X. P. Wang, Comm. Math. Phys. **131**, 109 (1990).
  - [23] R. Ma, M. E. Tai, P. M. Preiss, W. S. Bakr, J. Simon, and M. Greiner, Phys. Rev. Lett. **107**, 095301 (2011); Y.-A. Chen, S. Nascimbene, M. Aidelsburger, M. Atala, S. Trotzky, and I. Bloch, *ibid.* 210405.
  - [24] R. Ketzmerick and W. Wustmann, Phys. Rev. E **80**, 021117 (2009); F. Platzer, F. Mintert, and A. Buchleitner, Phys. Rev. Lett. **105**, 020501 (2010); P. Doria, T. Calarco, and S. Montangero, *ibid.* **106**, 190501 (2011).
  - [25] C. Kasztelan, S. Trotzky, Y.-A. Chen, I. Bloch, I. P. McCulloch, U. Schollwöck, and G. Orso, Phys. Rev. Lett. **106**, 155302 (2011); M. J. Mark, E. Haller, K. Lauber, J. G. Danzl, A. J. Daley, and H.-C. Nägerl, Phys. Rev. Lett. **107**, 175301 (2011); I. Bloch, J. Dalibard, and S. Nascimbene, Nature Phys. **8**, 267 (2012).
  - [26] P. Plötz and S. Wimberger, Eur. Phys. J. D **65**, 199 (2011).